

# Nonlinear nonlocal multicontinua upscaling framework and its applications

Wing T. Leung\*    Eric T. Chung†    Yalchin Efendiev‡    Mary Wheeler§

October 1, 2018

## Abstract

In this paper, we discuss multiscale methods for nonlinear problems. We use recently developed multiscale concepts for linear problems and extend them to nonlinear problems. The main idea of these approaches is to use local constraints and solve problems in oversampled regions for constructing macroscopic equations. These techniques are intended for problems without scale separation and high contrast, which often occur in applications. For linear problems, the local solutions with constraints are used as basis functions. This technique is called Constraint Energy Minimizing Generalized Multiscale Finite Element Method (CEM-GMsFEM). GMSFEM identifies macroscopic quantities based on rigorous analysis. In corresponding upscaling methods, the multiscale basis functions are selected such that the degrees of freedom have physical meanings, such as averages of the solution on each continuum.

This paper extends the linear concepts to nonlinear problems, where the local problems are nonlinear. The main concept consists of: (1) identifying macroscopic quantities; (2) constructing appropriate oversampled local problems with coarse-grid constraints; (3) formulating macroscopic equations. We consider two types of approaches. In the first approach, the solutions of local problems are used as basis functions (in a linear fashion) to solve nonlinear problems. This approach is simple to implement; however, it lacks the nonlinear interpolation, which we present in our second approach. In this approach, the local solutions are used as a nonlinear forward map from local averages (constraints) of the solution in oversampling region. This local fine-grid solution is further used to formulate the coarse-grid problem. Both approaches are discussed on several examples and applied to single-phase and two-phase flow problems, which are challenging because of convection-dominated nature of the concentration equation. The numerical results show that we can achieve good accuracy using our new concepts for these complex problems.

## 1 Introduction

As multiscale methods for linear equations are getting matured, their extension to difficult nonlinear problems remain challenging. Many nonlinear problems have multiscale nature due to spatial and temporal scales. For example, the dynamics of multi-phase flow and transport in heterogeneous media varies over multiple space and time scales. In the past, many well-known linear and nonlinear upscaling tools have been developed (e.g., [2, 27, 3, 26, 15, 8, 10, 23, 1, 21, 35, 36, 49, 47, 4, 43, 14, 17, 12, 52, 5, 13, 40, 48, 55]). Single-phase upscaling methods include permeability upscaling [22, 54, 9, 44] and many multiscale techniques [2, 26, 15, 49, 47, 4, 43]). Nonlinear upscaling methods, e.g., known as pseudo-relative permeability approach [9, 45, 7], computes nonlinear relative permeability functions based on single cell two-phase flow computations. It is known that these nonlinear approaches lack robustness and they are processes dependent [24, 25]. To overcome these difficulties, one needs a better understanding of nonlinear upscaling methods, which is our goal.

---

\*ICES, University of Texas, Austin, TX, USA ([wleung@ices.utexas.edu](mailto:wleung@ices.utexas.edu))

†Department of Mathematics, The Chinese University of Hong Kong, Shatin, New Territories, Hong Kong SAR, China ([tschung@math.cuhk.edu.hk](mailto:tschung@math.cuhk.edu.hk))

‡Department of Mathematics & Institute for Scientific Computation (ISC), Texas A&M University, College Station, Texas, USA ([efendiev@math.tamu.edu](mailto:efendiev@math.tamu.edu))

§ICES, University of Texas, Austin, TX, USA ([mfw@ices.utexas.edu](mailto:mfw@ices.utexas.edu))

Nonlinear upscaling methods can be traced back to nonlinear homogenization [51, 30]. The main idea of nonlinear homogenization is to formulate coarse-grid equations based on nonlinear local problems formulated in each coarse block. Some examples include p-Laplacian, pseudo-elliptic equations, and parabolic equations [30]. In these approaches, the local problems are solved with periodic boundary conditions and some constraints on averages of the solutions or gradients. In non-periodic cases, these methods are extended by solving local problems in coarse block subject to some boundary conditions. Because of nonlinearity, these local problems need to be solved for all possible average values, which can make the computations expensive. One can compute the upscaled fluxes on-the-fly using the values at previous iteration or previous time. These approaches are limited to problems without high contrast and scale separation. Our goal is to extend these approaches to problems with high contrast and non-separable scales. *The main novel components of our approach* is introducing multiple macroscopic variables for each coarse-grid block, formulating appropriate local constrained problems that determine the downscaling map; formulating macroscopic equations.

In computational mechanics literature, there has been a great deal of research dedicated to nonlinear upscaling methods, which include generalized continuum theories (e.g., [32]), computational continua framework (e.g., [39]), and other approaches. Multiscale enrichment method based on the partition of unity ([41, 42]) combine the linear and non-linear homogenization theory with the partition of unity method to handle the problems with inseparable fine and coarse scales. Computational continua ([39, 33]), which use nonlocal quadrature to couple the coarse scale system stated on a unions of some disjoint computational unit cells, are introduced for non-scale-separation heterogeneous media. In [38, 37, 34], the authors further enhance the method by combining the computational continua with model reduction technique. Originally, the computational continua approaches were developed to overcome the limitations of higher-order homogenization models and generalized continuum theories, namely, the need for higher-order finite element continuity, additional degrees of freedom, and nonclassical boundary conditions. Though there are some similarities, our proposed approaches differ from computational continua framework. Our approach explores the localization of high-contrast (with respect to the coarse-mesh size) features by introducing additional degrees of freedom (continua) and using oversampled regions. In future, we plan to use some ingredients of computational continua approaches in improving our approach and in making it more applicable to computational materials.

To design the new upscaled model, we use the concept of non-local multi-continuum (NLMC). The main idea of NLMC derives from Constraint Energy Minimizing Generalized Multiscale Finite Element Method (CEM-GMsFEM) [19, 20, 16]. CEM-GMsFEM identifies the degrees of freedom which can not be localized and then construct multiscale basis functions with support in the oversampled regions. However, the degrees of freedom in CEM-GMsFEM, in general, do not have physical meanings since they are coordinates in the multiscale space. In order to obtain an upscaled model, we design multiscale basis functions such that the degrees of freedom represent the average of the solutions. As a result, the coarse-grid model is an equation for the solutions averaged over each continua. In this paper, we extend this idea to nonlinear equations.

To extend the concept of NLMC to nonlinear equations, we first identify macroscopic quantities for each coarse-grid block. These variables are typically found via local spectral decomposition and represent the features that can not be localized (similar to multicontinua variables [6, 46, 53, 50]). Next, we consider local problems formulated in the oversampled regions with constraints. These local problems allow identifying the downscaling map from average macroscopic quantities to the fine-grid variables. By imposing the constraints for each continuum variable via the source term, we define effective fluxes and the homogenized equation. Using the local solutions in the oversampled regions with constraints allows localizing the global downscaled map, which provides an accurate representation of the solution; however, it is expensive as it involves solving the global problem. By using the constraints in the oversampled regions, we can guarantee the proximity between the global and local downscaled maps for a given set of oversampled constraints.

The resulting homogenized equation significantly differs from standard homogenization. First, there are several variables per coarse block, which represent each continuum. Secondly, the local problems are formulated in oversampled regions with constraints. Finally, the nonlinear homogenized fluxes depend on all averages in oversampled regions, which bring non-local behavior for the equation. These ingredients are needed to perform upscaling in the absence of scale separation and high contrast.

In summary, our nonlinear nonlocal multicontinua approach has the following steps.

- For each coarse-grid block, identify coarse-grid variables (continua) and associated quantities. This is typically done via some local spectral problems and describes the quantities that can not be localized.

- Define local problems in oversampled regions with constraints. The constraints are given for each continua variables over all coarse-grid blocks. Local problems use specific source terms and boundary conditions, which allow localizing the global downscaled map and identifying effective fluxes. This step gives a downscaling from average continua to the fine-grid solution.
- The formulation of the coarse-grid problem. We seek the coarse-grid variables such that the downscaled fine-grid solution approximately solves the global problem in a weak sense. The weak sense is defined via specific test functions, which are piecewise constants in each continua. This provides an upscaled model.

We consider two types of methods. First, we call linear interpolation and the second is non-linear interpolation. In the first approach, we seek the solution in the form

$$w = \sum_{i,j} w_i^j \phi_i^j,$$

where  $\phi_i^j$  are multiscale basis functions for coarse cell  $i$  and for continua  $j$  defined in the oversampled region. This approach is simpler as one uses linear approximation of the solution. However, because of the nonlinearity, the nonlinear approximation is needed (see [29, 31, 30]). In [30], the authors propose such approach for pseudomonotone equations (similar to homogenization). In our problem, we present a nonlinear interpolation (we refer as nonlinear nonlocal multicontinua). In this approach, the solution is sought as a nonlinear map, which approximated  $w_i^j$  from neighboring cells in a nonlinear fashion, which is defined via local problems. The local problem provides a nonlinear map from coarse-grid macroscopic variables to the fine-grid solution. This mapping is used to construct macroscopic equations. We use non-locality and multi-continua to address the cases without scale separation and high contrast.

As one of the numerical examples, we consider two-phase flow and transport, though our approach can be applied to a wide range of problems. Two-phase flow and transport is one of challenging problems, where many attempts are made to study it. Typical approaches include pseudo-relative permeability approach, also known as multi-phase upscaling, where the relative permeabilities are computed based on local two-phase flow simulations. It is known that these approaches are process dependent. Our approach provides a novel upscaling, which shows that each coarse-grid block needs to contain several average pressures and saturations and, moreover, these coarse-grid relative permeabilities are non-local and depend on saturations and pressures of neighboring cells. This model provides a new way to look at two-phase flow equations and can be further used in different modeling purposes.

The paper is organized as follows. In the next section, Section 2, we present some preliminaries and discuss main concepts used for linear problems. Section 3 is devoted to a general concept of nonlinear upscaling and this is discussed on several examples. In Section 4, we present the linear interpolation based approach and numerical results for multi-phase flow and transport. Though the paper's main focus is on nonlinear interpolation, the linear interpolation approach is practical for many applications. In Section 5, we present the nonlinear approach for multi-phase flow and corresponding numerical results.

## 2 Preliminaries

We consider a general nonlinear system of the form

$$\partial_t U + G(x, t, U, \nabla U) = g. \quad (1)$$

In general,  $U$  is a vector-valued function and  $g(x, t)$  is the source term.  $G$  is assumed to be heterogeneous in space (and time, in general), which are resolved on the fine grid (see Figure 1 for fine and coarse grid illustrations). Our objective is to derive coarse-grid equations. First, we discuss some examples for (1).

**Example 1.** Nonlinear (pseudomonotone) parabolic equations, where  $G(x, t, U, \nabla U) := \text{div} \kappa(x, t, U, \nabla U)$ .

**Example 2.** Hyperbolic equations, where  $G(x, t, U, \nabla U) := v(x) \cdot \nabla G(x, U)$  and  $U$  is a scalar function and  $v$  is a vector valued function. For example,  $v = -\kappa(x) \nabla p$  and  $\text{div}(v) = q$ , as in Darcy's flow.

**Example 3.** Hamilton-Jacobi equations, where  $G(x, t, U, \nabla U) := G(x, \nabla U)$  and  $U$  is a scalar function.

**Example 4.** One of our objective in this paper is to address the upscaling of multi-phase flow, which is a challenging problem. In this case, the model equations have the following form. The two-phase flow equations are derived by writing Darcy's flow for each water ( $\alpha = w$ ) and oil ( $\alpha = o$ ) phases and the mass conservation as follows

$$\begin{aligned} u_\alpha &= -\lambda_{rw}(S_w)\kappa(x)\nabla p \\ \nabla \cdot (u_t) &= q_p, \quad \partial_t S_\alpha + \nabla \cdot (u_\alpha) = q. \end{aligned} \tag{2}$$

Here,  $u_\alpha$  is the Darcy velocity of the phase  $\alpha$ ,  $u_t = \sum_\alpha u_\alpha$ ,  $S_\alpha$  is the saturation of the phase  $\alpha$ , and  $\lambda_{r\alpha}$  is the relative mobility of the phase  $\alpha$ . By denoting the saturation of the water phase via  $S = S_w$ , we can write the equations in the following way

$$\begin{aligned} -div(\lambda(S)\kappa\nabla p) &= q_p \\ \partial_t S + \nabla \cdot (uf(S)) &= q, \quad u = -\kappa\nabla p. \end{aligned} \tag{3}$$

The special case of the two-phase flow consists of single-phase flow

$$\begin{aligned} -div(\kappa\nabla p) &= q_p \\ \partial_t S + \nabla \cdot (uS) &= q, \quad u = -\kappa\nabla p. \end{aligned} \tag{4}$$

## 2.1 Overview of NLMC for linear problems

In this section, we will give a brief overview of the NLMC method for linear problems [18]. Our goal is to summarize the key ideas in linear NLMC and motivate the ideas in the extension of it to the nonlinear NLMC in the next section. To be specific, we will consider a model parabolic equation with a heterogeneous coefficient, namely,

$$\frac{\partial u}{\partial t} - div(\kappa\nabla u) = g, \quad \text{in } \Omega \times [0, T], \tag{5}$$

with appropriate initial and boundary condition, where  $\kappa$  is the heterogeneous field,  $g$  is a given source,  $\Omega$  is the physical domain and  $T > 0$  is a fixed time.

The NLMC upscaled system is defined on a coarse mesh,  $\mathcal{T}^H$ , of the domain  $\Omega$ . We write  $\mathcal{T}^H = \bigcup\{K_i \mid i = 1, \dots, N\}$ , where  $K_i$  denotes the  $i$ -th coarse element and  $N$  denotes the number of coarse elements in  $\mathcal{T}^H$ . For each coarse element  $K_i$ , we will identify multiple continua corresponding to various solution features. This can be done via a local spectral problem or a suitable weight function. The upscaled parameter is defined using multiscale basis functions. For each coarse element  $K_i$  and each continuum within  $K_i$ , we will construct a multiscale basis function whose support is an oversampled region  $K_i^+$ , which is obtained by enlarging the coarse block  $K_i$  by a few coarse grid layers. See Figure 1 for an illustration of coarse grid and oversample region. In particular, a structured coarse grid is shown with boundaries of coarse elements are denoted blue. A coarse cell  $K$  is denoted red and its oversampled region  $K^+$  obtained by enlarging  $K$  by two coarse grid layers is denoted green.

Now we will specify the definition of continuum. For each coarse block  $K_i$ , we will identify a set of continua which are represented by a set of auxiliary basis functions  $\phi_i^j$ , where  $j$  denotes the  $j$ -th continuum. There are multiple ways to construct these functions  $\phi_i^j$ . One way is to follow the idea proposed in CEM-GMsFEM [19]. In this framework, the auxiliary basis functions  $\phi_i^j$  are obtained as the dominant eigenfunctions of a local spectral problem defined on  $K_i$ . These eigenfunctions can capture the heterogeneities and the contrast of the medium. The resulting solution of the upscaled system corresponds to the moments of the true solution with respect to these eigenfunctions. Another way is to follow the framework in the original NLMC method [18], designed for flows in fractured media, which can be easily modified for general heterogeneous media. In this approach, one identifies explicit information of fracture networks. The auxiliary basis functions  $\phi_i^j$  are piecewise constant functions, namely, they equal one within one fracture network and zero otherwise. The resulting solution of the upscaled system corresponds to the average of the solution on fracture networks, which can be regarded as one of the continua. Finally, one can generalize the previous approach to construct other auxiliary basis functions. In particular, we can define  $\phi_i^j$  to be characteristic functions of some regions  $K_i^{(j)} \subset K_i$ . These regions  $K_i^{(j)}$  can be chosen to reflect various properties of the medium. For instances, one

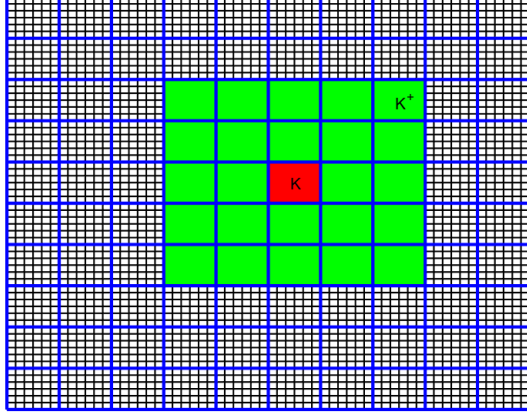


Figure 1: Illustration of coarse and fine meshes as well as oversampled regions. The region  $K^+$  (in Green) is an oversampled region corresponding to the coarse block  $K$  (in red).

can choose  $K_i^{(j)}$  to be the region in which the medium has a certain range of values. We will consider this last choice in this paper.

Once the auxiliary basis functions  $\phi_i^j$  are specified, we can construct the required basis functions. The idea generalizes the original energy minimization framework in CEM-GMsFEM. Consider a given coarse element  $K_i$  and a given continuum  $j$  within  $K_i$ . We will use the corresponding auxiliary basis function  $\phi_i^j$  to construct our required multiscale basis function  $\psi_i^j$  by solving a problem in an oversampled region  $K_i^+$ . Specifically, we find  $\psi_i^j \in H_0^1(K_i^+)$  and  $\mu \in V_{aux}$  such that

$$\begin{aligned} \int_{K_i^+} \kappa \nabla \psi_i^j \cdot \nabla v + \int_{K_i^+} \mu v &= 0, \quad \forall v \in H_0^1(K_i^+), \\ \int_{K_\ell} \psi_i^j \phi_m^\ell &= \delta_{j\ell} \delta_{im}, \quad \forall K_\ell \subset K_i^+, \end{aligned} \quad (6)$$

where  $\delta_{im}$  denotes the standard delta function and  $V_{aux}$  is the space spanned by auxiliary basis functions. We remark that the function  $\mu$  serves as a Lagrange multiplier for the constraints in the second equation of (6). We also remark that the basis function  $\psi_i^j$  has mean value one on the  $j$ -th continuum within  $K_i$  and has mean value zero in all other continua in all coarse elements within  $K_i^+$ . In practice, the above system (6) is solved in  $K_i^+$  using a fine mesh, which is typically a refinement of the coarse grid. See Figure 1 for an illustration.

Now, we can derive the NLMC upscaled system. As an illustration of the concept, we consider a forward Euler method for the time discretization of (5). At the  $n$ -th time step, the solution vector is denoted by  $U^n$ , where each component of  $U^n$  represents the average of the solution on a continuum within a coarse element. We note that the size of this vector is  $\sum_{i=1}^N L_i$ , where  $L_i$  is the number of continua in  $K_i$ . The upscaled stiffness matrix  $A_T$  is defined as

$$(A_T)_{jm}^{(i,\ell)} = a(\psi_j^i, \psi_m^\ell) := \int_{\Omega} \kappa \nabla \psi_j^i \cdot \nabla \psi_m^\ell, \quad (7)$$

and the upscaled mass matrix  $M_T$  is defined as

$$(M_T)_{jm}^{(i,\ell)} = \int_{\Omega} \psi_j^i \psi_m^\ell. \quad (8)$$

Finally, the NLMC system is written as

$$M_T(U^{n+1} - U^n) + \Delta t A_T U^n = \Delta t G^n \quad (9)$$

where the components of the vector  $G^n$  are defined as  $\int_{\Omega} g(\cdot, t_n) \phi_i^j$  and  $t_n$  is the time at the  $n$ -th time step. We remark that the nonlocal connections of the continua are coupled by the matrices  $A_T$  and  $M_T$ . We also remark that the local computation in (6) results from a spatial decay property of the multiscale basis function, see [19, 20, 16] for the theoretical foundation.

### 3 Nonlinear non-local multicontinua model

#### 3.1 General concept

We will first present some general concept of our nonlinear NLMC. We consider the following nonlinear problem

$$U_t + G(x, U, \nabla U) = g, \quad (10)$$

where  $G$  has a multiscale dependence with respect to space (and time, in general).

To formulate the coarse-grid equations in the time interval  $[t_n, t_{n+1}]$ , we first introduce coarse-grid variables  $U_i^{n,j}$ , where  $i$  is the coarse-grid block,  $j$  is a continuum representing the coarse-grid variables, and  $n$  is the time step (cf. [18]). As we noted that the continuum plays a role of a macroscopic variable, which can not be localized. For each coarse-grid block  $i$ , we need several coarse-grid variables, which will be indexed by  $j$ . In this paper, we will consider two types of interpolation for multiscale degrees of freedom. The first approach is called linear interpolation, which constructs approximate solution  $U_H^n$  at the time  $t_n$  as

$$U_H^n = \sum_{i,j} U_i^{n,j} \psi_i^j,$$

where  $\psi_i^j$  are multiscale basis functions, which are defined via local constrained problems formulated in the oversampled regions. These basis functions are possibly supported in the oversampled regions and the resulting coarse-grid equations will be nonlinear and non-local when projected to the appropriate test spaces. The values of  $U_i^{n,j}$  are computed via the variational formulation using an explicit or implicit discretization of time

$$(U_H^{n+1}, V_H) - (U_H^n, V_H) + \Delta t(G(x, U_H^L, \nabla U_H^L), V_H) = \Delta t(g, V_H), \quad \forall V_H, \quad (11)$$

where  $L = n$  or  $L = n + 1$  depending whether explicit or implicit discretization is used, and  $V_H$  denotes test functions. Here,  $(\cdot, \cdot)$  denotes usual  $L^2$  inner product. As for the test space, one can use the multiscale space spanned by  $\psi_i^j$  or the auxiliary basis functions  $\phi_i^j$ . This linear approach is simpler to use; however, it ignores the nonlinear interpolation, which is important for nonlinear homogenization and numerical homogenization [51, 30].

Next, we describe the nonlinear approach, which we refer as nonlinear nonlocal multicontinuum approach. In this case, the solution is sought as a nonlinear interpolation of the degrees of freedom  $U_i^{n,j}$  defined in the oversampled region. More precisely, we compute a downscale function using the given solution values  $U_i^{n,j}$  by solving a constrained problem in the oversampled regions. Mathematically, this downscale function  $U_h^n$  can be written as a function of all values  $U_i^{n,j}$ , namely,

$$U_h^n = \mathcal{F}(U^n),$$

where  $\mathcal{F}$  is a nonlinear map and  $U^n$  is a vector containing all values  $\{U_i^{n,j}\}$ . The nonlinear map is computed by solving the local problem (cf. (14)), and the function  $U_h^n$  is glued together from local downscaled maps. Once this map is defined, we seek all coarse-grid macroscopic variables  $\{U_i^{n,j}\}$  such that the downscaled fine-grid solution  $U_h^n$  solves the global problem in a variational setting. The test functions are defined for each degrees of freedom in the form of piecewise constants or piecewise functions, in for example a finite volume or Petrov Galerkin setting. More precisely, the coarse-grid system has the form

$$(U_h^{n+1}, V_H) - (U_h^n, V_H) + \Delta t(G(x, U_h^L, \nabla U_h^L), V_H) = \Delta t(g, V_H), \quad (12)$$

for all suitable test functions  $V_H$ . Here,  $L = n$  or  $L = n + 1$  can be used for explicit or implicit discretization. The test functions are chosen to be piecewise polynomials or auxiliary basis functions  $\phi_i^j$ . We remark that the dimension of the test space is chosen to be the dimension of the coarse-grid macroscopic variables.

### 3.2 Nonlinear nonlocal multicontinuum approach

In this section, we give some details of our nonlinear nonlocal multicontinuum approach, in general, and then present some examples. The illustration is given in Figure 2. In later sections, we present a detailed application to two-phase flow equations.

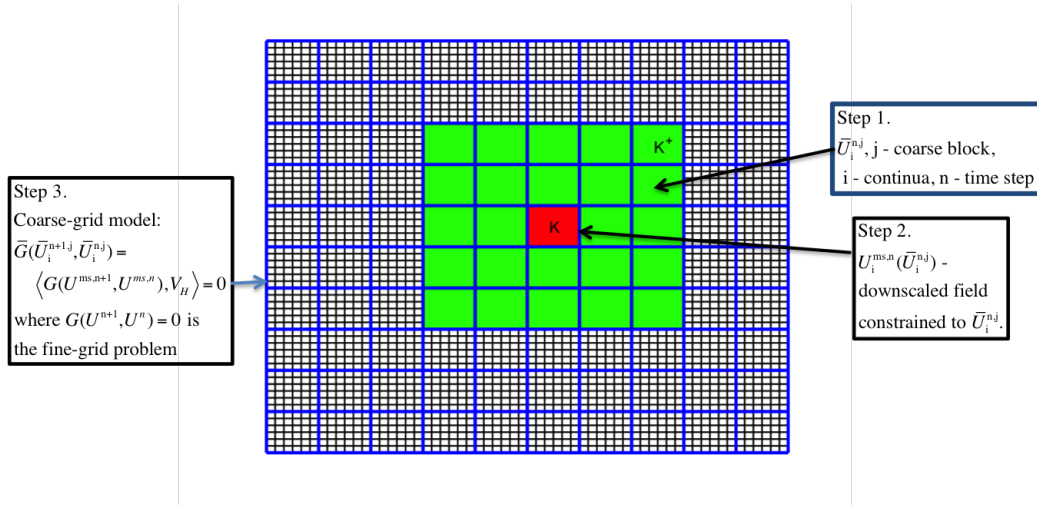


Figure 2: Illustration of the steps.

**Step 1. Defining coarse-grid variables.** The first step involves defining macroscopic variables. In our cases, we will define them by  $U_j^{n,i}$ , where  $i$  is the coarse-grid block,  $j$  is the continua, and  $n$  is the time step. These variables in our applications will be defined by prescribing averages to subregions, which can have a complex shapes (for example, fracture regions). The equation for  $U_j^{n,i}$ , in general, will have a form

$$\bar{U}_j^{n+1,j} - \bar{U}_j^{n,j} + \bar{G}_i^j(\bar{U}^L) = 0, \quad (13)$$

where  $L = n$  or  $L = n + 1$  for explicit or implicit discretizations. The operator  $\bar{G}_i^j$  is determined respect to the given continuum  $j$  and coarse element  $i$ , and contains information from the source term and the time step size  $\Delta t$ . In (13), we use  $\bar{U}^L$  to denote the vector consisting of all macroscopic quantities  $U_i^{L,j}$  for all  $i$  and  $j$ . The operator  $\bar{G}_i^j$  is obtained by solving local problems on an oversampled region corresponding to  $K_i$ . To define (13), we next discuss local problems.

**Step 2. Local solves for generic constraints.** The computation of  $\bar{G}_i^j$  requires solutions of constrained local nonlinear problems. Here we present a general formulation. We consider  $i$  to be the index for a coarse element  $K_i$  or a coarse neighborhood  $\omega_i$ , which is defined for a coarse node  $i$  by

$$\omega_i = \bigcup \{K \in \mathcal{T}^H : x_i \in \bar{K}\}.$$

The choice of  $K_i$  or  $\omega_i$  depends on the global coarse grid discretization. For example, with finite volume or Petrov Galerkin formulation, we choose  $K_i$ , while for continuous Galerkin formulation, we choose  $\omega_i$ . In this part, we present the steps using  $\omega_i$ . The required local nonlinear problem will be solved on  $\omega_i^+$ , which is an oversampled region obtained by enlarging  $\omega_i$  a few coarse grid layers. We let  $c := \{c_m^{(l)}\}$  be a set of scalar values, where  $m$  denotes the  $m$ -th coarse element in the oversampled region  $\omega_i^+$  and  $l$  denotes the  $l$ -th continuum within  $K_m \subset \omega_i^+$ . The local problem is solved by finding a function  $N_{\omega_i}(x; c)$  given by

$$G(x, N_{\omega_i}(x; c), \nabla N_{\omega_i}(x; c)) = \sum_{m,l} \mu_{i,m}^{(l)}(c) I_{K_m^{(l)}} \text{ in } \omega_i^+ \quad (14)$$

with constraints

$$\int_{\omega^+} N_{\omega_i}(x; c) I_{K_m^{(l)}}(x) = c_m^{(l)}.$$

Here,  $I_{K_m^{(l)}}(x)$  is an indicator function for the region  $K_m^{(l)}$  defined for the continua  $l$  within coarse block  $m$ . We remark that the values  $\mu_{i,m}^{(l)}(c)$  play the role of Lagrange multipliers for the constraints. We notice that  $N_{\omega_i}$  depends on all constraints in the oversampled region. In general, one can also impose constraints on the gradients of  $N_{\omega_i}$  and the constraint function can have a complex form. We remark that the problem (14) requires a boundary condition, which is problem dependent. We will discuss it later. Our main message is that the local problems with constraints are solved in oversampled region and involves several coarse-grid variables for each coarse block. For the precise formulation, the values  $\{c_m^{(l)}\}$  will be chosen as the macroscopic variables.

**Discussion on localization.**

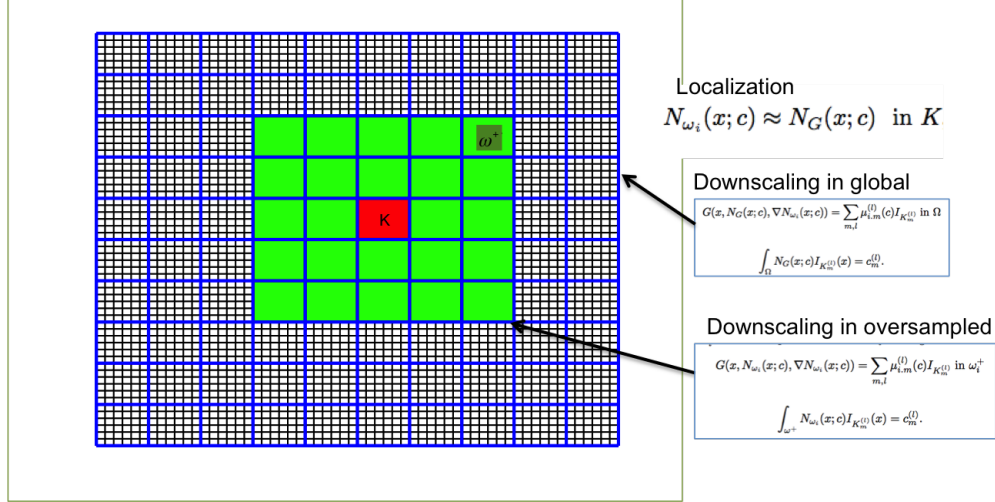


Figure 3: Illustration of the localization.

Next, we discuss the idea behind the localization principle stated above (see Figure 3 for illustration). For this reason, we first define the global downscaling operator,  $N_G(x; c)$ , which solves the global problem with constraints

$$G(x, N_G(x; c), \nabla N_G(x; c)) = \sum_{m,l} \mu_{i,m}^{(l)}(c) I_{K_m^{(l)}} \text{ in } \Omega \quad (15)$$

with constraints

$$\int_{\Omega} N_G(x; c) I_{K_m^{(l)}}(x) = c_m^{(l)}.$$

The boundary conditions are taken as the original global boundary conditions. For our localization, we desire that the local downscaled solution,  $N_{\omega_i}(x; c)$  in  $K$  (target coarse block) defined in (14), is approximately the same as  $N_G$  restricted to  $K$  for the same constraint values as the global problem in  $\omega_i^+$ . I.e.,

$$N_{\omega_i}(x; c) \approx N_G(x; c) \text{ in } K,$$

where  $c$  values coincide in  $\omega_i^+$ . This property allows solving local nonlinear problems instead of the global problem without sacrificing the accuracy and defining correct upscaled coefficients. This desired property can be shown for monotone elliptic equations using zero Dirichlet boundary conditions on  $\partial\omega_i^+$ . For more complex nonlinear system, one needs to also use appropriate boundary conditions on  $\partial\omega_i^+$  to achieve this property.

**Step 3. Defining coarse-grid model.** The upscaled flux  $\overline{G}_i^j$  is defined by substituting the downscaled global solution corresponding to the constraints given by  $c$  and multiplying it by test functions. For this procedure, one first defines a global fine-grid downscaled field that is constrained. The equation (14) defines local fine-grid fields constrained to macroscopic variables in oversampled regions. In general, one needs to “glue” together a global downscaled solution, which approximates the global problem in a weak sense. A



simple approach to glue together is to use partition of unity functions,  $\chi_{\omega_i}$  for each region  $\omega_i$ . Then,

$$\mathcal{F}(\bar{U}) = \sum_i N_{\omega_i} \chi_{\omega_i}.$$

In some discretization scenarios (e.g., finite volume, Discontinuous Galerkin,...), it is not necessary to glue together in order to obtain a global fine-grid field. In the proposed NLMC approach, our coarse-grid formulation uses “finite volume” type approximation and we will not need to glue local approximations. In this case,

$$\mathcal{F}(\bar{U}) = N_{\omega_i} \text{ and } \nabla \mathcal{F}(\bar{U}) = \nabla N_{\omega_i} \text{ on } E_i. \quad (16)$$

where  $E_i$  is a coarse edge for the coarse grid. In general, we can write it as  $\mathcal{F}(\bar{U}) = N_{\omega_i}$  in all local fine-grid blocks, and the following variational formulation

$$\left( \frac{\partial}{\partial t} \mathcal{F}(\bar{U}), V_H \right) + (G(x, \mathcal{F}(\bar{U}), \nabla \mathcal{F}(\bar{U})), V_H) = (g, V_H), \quad (17)$$

where  $V_H$  are test functions. In this setup,

$$(G(x, \mathcal{F}(\bar{U}), \nabla \mathcal{F}(\bar{U})), V_H) = (\bar{G}(x, \bar{U}), V_H).$$

The above equation can formally be thought as

$$\frac{\partial}{\partial t} \mathcal{M}(\bar{U}) + \mathcal{G}(\bar{x}, \bar{U}) = \bar{g}.$$

The time discretization of Equation (17) can be written as

$$(\mathcal{F}(\bar{U}^{n+1}), V_H) - (\mathcal{F}(\bar{U}^n), V_H) + \Delta t (G(x, \mathcal{F}(\bar{U}^L), \nabla \mathcal{F}(\bar{U}^L)), V_H) = \Delta t (g, V_H), \quad (18)$$

where  $L = n$  or  $L = n + 1$  for explicit or implicit discretizations. In general, the downscaling operator has the following property

$$(\mathcal{F}(\bar{U}^L), V_H) \approx (\bar{U}^L, V_H), \quad \text{or} \quad (\mathcal{F}(\bar{U}^L), V_H) = (\bar{U}^L, V_H) \quad (19)$$

which simplifies the computations. In the latter situation, the mass matrix  $\mathcal{M}$  is diagonal. In addition,

$$(\mathcal{F}(\bar{U}^L), V_h) \approx (U_h^L, V_h), \quad (20)$$

where  $U_h^L$  is a fine-scale field and  $\bar{U}^L$  is the corresponding coarse-grid average. The equation (20) states that if we use the average of the fine-scale field to re-construct it, the resulting approximation remains close to the original fine-scale field. We remark that the operator  $\bar{G}_i^j$  in (13) is obtained using (18). More precisely, we have

$$\bar{G}_i^j := \Delta t (G(x, \mathcal{F}(\bar{U}^L), \nabla \mathcal{F}(\bar{U}^L)), V_H) - \Delta t (g, V_H)$$

by using a test function  $V_H$  corresponding to region  $i$  and continuum  $j$ .

Next, we present some more concrete constructions for some cases, listed in Section 2.

**Example 1.** In this example, we consider a class of nonlinear (pseudomonotone) parabolic equations with  $G = \text{div}(k(x, U, \nabla U))$ , where  $k$  is a heterogeneous function in  $x$ , and in general, also in  $U$  and  $\nabla U$ . We will consider a continuous Galerkin discretization in space on a coarse grid and explicit Euler discretization in time. Let  $c = \{U_i^{n,j}\}$  be a set of macroscopic variables at the time  $t_n$ . In particular,  $U_i^{n,j}$  denotes the mean value of the solution on continuum  $j$  within coarse element  $i$  at time  $t_n$ . On an oversampled region  $\omega_i^+$ , we find a function  $N_{\omega_i}$  on the fine grid such that

$$G(x, N_{\omega_i}, \nabla N_{\omega_i}) = \sum_{K_m^{(l)} \subset \omega_i^+} \mu_m^{(l)}(c) I_{K_m^{(l)}} \quad \text{in } \omega_i^+$$

subject to the following constraints

$$\begin{aligned} \int_{\omega_i} N_{\omega_i}(x) I_{K_m^{(l)}}(x) &= U_m^{n,l}, \quad \forall K_m^{(l)} \subset \omega_i, \\ \int_{\omega_i} N_{\omega_i}(x) I_{K_m^{(l)}}(x) &= 0, \quad \forall K_m^{(l)} \subset \omega_i^+ \setminus \omega_i. \end{aligned}$$

We remark that  $\mu_m^{(l)}$  plays the role of Lagrange multiplier. The above problem is solved using the Dirichlet boundary condition on  $\partial\omega_i^+$ . We can set  $N_{\omega_i}$  equals to zero on  $\partial\omega_i^+$ , and this choice is motivated by the decay property of multiscale basis functions in CEM-GMsFEM. Then we can define a global fine scale function by

$$U_h^n = \sum_i N_{\omega_i} \chi_{\omega_i}$$

where  $\{\chi_{\omega_i}\}$  are suitable partition of unity functions, where we notice that the values of  $N_{\omega_i}$  within  $\omega_i^+ \setminus \omega_i$  are not used. Using the global downscale function  $U_h^n$  and suitable test functions, we can derive a coarse grid scheme. We note that the upscaled model has the form (17).

**Example 2.** In this example, we consider a class of hyperbolic equations, where  $G(x, t, U, \nabla U) := v(x) \cdot \nabla G(x, U)$  and  $U$  is a scalar function and  $v$  is a vector valued function. For example,  $v = -\kappa(x) \nabla p$  and  $\text{div}(v) = q$ , as in Darcy's flow. We will consider a finite volume type discretization in space on a coarse grid and explicit Euler discretization in time. Let  $c = \{U_i^{n,j}\}$  be a set of macroscopic variables at the time  $t_n$ . Same as above,  $U_i^{n,j}$  denotes the mean value of the solution on continuum  $j$  within coarse element  $i$  at time  $t_n$ . On an oversampled region  $K_i^+$ , we find a function  $N_{K_i}$  on the fine grid such that

$$G(x, \nabla N_{K_i}) = \sum_{K_m^{(l)} \subset K_i^+} \mu_m^{(l)}(c) I_{K_m^{(l)}} \quad \text{in } K_i^+$$

subject to the following constraints

$$\int_{K_i^+} N_{\omega_i}(x) I_{K_m^{(l)}}(x) = U_m^{n,l}, \quad \forall K_m^{(l)} \subset K_i^+.$$

We remark that  $\mu_m^{(l)}$  plays the role of Lagrange multiplier. The above problem is solved using the standard inflow boundary condition on the inflow part of  $\partial K_i^+$ . We can set  $N_{K_i}$  equals to zero to the value  $\{U_i^{n,j}\}$  chosen by upwinding. Then we can define a global fine scale function by

$$U_h^n = \sum_i N_{K_i} \chi_{K_i^+}$$

where  $\{\chi_{K_i^+}\}$  are suitable partition of unity functions for the overlapping partition  $\{K_i^+\}$ . We remark that this global downscale function  $U_h^n$  preserves the mean values, namely,

$$\frac{1}{|K_i^{(j)}|} \int_{K_i^{(j)}} U_h^n = U_i^{n,j}.$$

Using the global downscale function  $U_h^n$  and suitable test functions, we can derive a coarse grid scheme. For the test functions, we use  $\{I_{K_m^{(l)}}(x)\}$ , for all  $m, l$ . Hence, we obtain

$$U_i^{n+1,j} = U_i^{n,j} - \Delta t \int_{K_i^{(j)}} G(x, \nabla U_h^n) + \Delta t \int_{K_i^{(j)}} g, \quad \forall i, j. \quad (21)$$

We note that this upscaled model has the form (17). We also note that the number of unknowns is the same of number of equations.

**Example 3.** For this case, the local problem can be formulated as follows. On an oversampled region  $K_i^+$ , we find a function  $N_{K_i}$  on the fine grid such that

$$G(x, \nabla N_{K_i}) = \sum_{K_m^{(l)} \subset K_i^+} \mu_m^{(l)}(c) I_{K_m^{(l)}} \quad \text{in } K_i^+$$

subject to the following constraints

$$\int_{K_i^+} N_{\omega_i}(x) I_{K_m^{(l)}}(x) = U_m^{n,l}, \quad \forall K_m^{(l)} \subset K_i^+.$$

Similar to Example 2, the upscaled model has the form (17) and (21).

In summary, the local problems involve original local problems with constraints formulated in the oversampled regions. The source term constants represent the homogenized fluxes and their dependence on averages of solutions and gradients are the functional form of the equations.

### 3.2.1 RVE-based extension of the method

The proposed concept can also be used for problems with scale separation. A typical example is a fractured media, where the fracture distributions are periodic or possess some scale separation. In this case, we do not use the oversampling based local problems and simply use local problems in RVE. To be more precise, Step 1 remains the same as before, which involves identifying local multicontinua variables in each coarse-grid block.

In Step 2, we solve the local problem (14) in RVE subject to the constraints. The main difference is that we use only the constrained in the target coarse-grid block. Thus, there are fewer constraints and the problem is localized to the target coarse block.

Once the local solves are defined, via periodicity, we extend the local solution to the  $\omega_i$  and use this extension to compute the effective flux. This construction is similar to e.g., [30] or MsFEM using RVE [28].

## 4 Linear Approach

In this section, we will focus on the linear approach (c.f. Section 3), and present some numerical results.

### 4.1 Linear transport

In this section, we will present some numerical results for the linear transport equation with a given velocity. More precisely, we consider

$$\partial_t S + \nabla \cdot (uS) = q \text{ in } \Omega$$

where  $u \in H(\text{div}, \Omega)$  is a given divergence-free velocity field with  $u \cdot n = 0$  on  $\partial\Omega$ . We take  $\Omega = [0, 1]^2$ , and the velocity field  $u$  is shown in Figure 4. The coarse grid size  $H = 1/20$ , and we use a single continuum model. In Table 1, we present an error comparison between our upscaling method and the standard finite volume method.

The derivation of the upscaled system follows the ideas in Section 2.1. For each coarse element  $K_i$ , we solve the following system in an oversampled region  $K_i^+$ :

$$\nabla \cdot (u\psi_i) + \mu = 0 \tag{22}$$

to obtain a basis function  $\psi_i$ . The above system is equipped with the constraints

$$\int_{K_j} \psi_i = \delta_{ij}. \tag{23}$$

We remark that  $\mu$  is a piecewise constant function, and plays the role of Lagrange multiplier. We notice that the upscaled system has the form (9). In practice, one can add artificial diffusion in (22) in order to obtain a stable numerical solution, and use zero Dirichlet boundary condition. We remark that one can use other boundary conditions, see Section 3.2.

By using the standard finite volume method, the relative  $L^2$  error is 27.78% at the final time  $T = 1$ . From Table 1, we see that our upscaling method provides much better approximations, where "# layer" standards for the number of layers used in the oversampling domains. When # layer equals  $\infty$ , it means that the oversampling domain is the whole physical domain. In Figure 5, we show the snapshots of the solution at  $T = 1$ . From this figure, we observe that the solution computed with CEM provides a good approximation, particularly, in saturated regions.

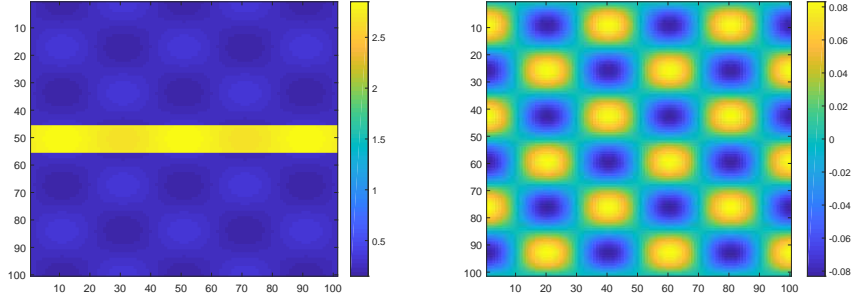


Figure 4: A velocity field  $u$ . Left:  $x_1$ -component. Right:  $x_2$ -component.

#layer	Errors
5	11.57%
7	7.73%
9	7.22%
$\infty$	6.91%

Table 1:  $L^2$  relative errors for our upscaling method. The relative error for standard finite volume scheme on the same grid is 27.78%.

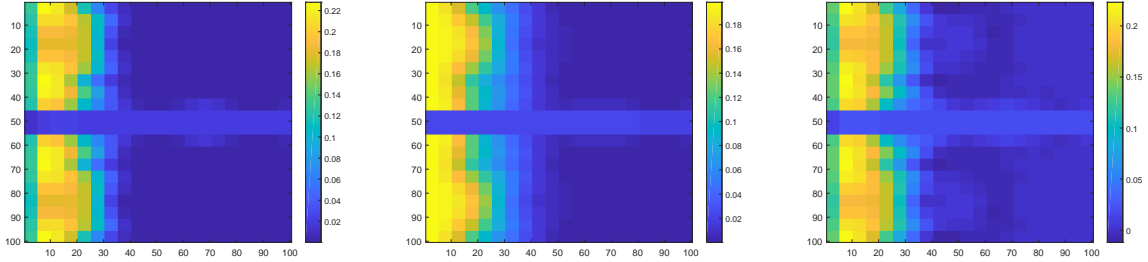


Figure 5: Snapshots of the solution at  $T = 1$ . Left: fine solution, Middle: finite volume solution, Right: upscale solution with 5 oversampling layers.

## 4.2 Single phase flow

In this section, we apply our method to a single phase flow problem which is described as follows:

$$\partial_t S_w + \nabla \cdot (u_w S_w) = q_w, \quad (24)$$

$$-\nabla \cdot (\kappa \nabla P_w) = q, \quad (25)$$

$$u_w = -\kappa \nabla P_w, \quad (26)$$

where we assume  $q$  is a function independent of time such that we can compute the velocity  $u_w$  in the initial time step and use the velocity to construct the basis function for saturation  $S_w$ .

For solving single phase flow problem, we can separate the computation process into two parts. Since Equations (25) and (26) are independent of saturation and the given source term is independent of time, we know that the velocity is independent of time. Therefore, we can decouple system of equation into two parts which are the Equations (25)-(26) and the Equation (24). The first part of the computation is computing the velocity and pressure by solving Equations (25) and (26) by Mixed Generalized Multiscale Finite Element Methods(MGMsFEM) [11]. The second part of the computation is computing the numerical solution for the saturation by solving Equation (24). Given a numerical velocity  $u_{ms}$ , Equation (24) is a standard linear transport equation. We can use the method discussed in Section 4.1 to construct the multiscale basis

function and then compute the numerical solution for saturation. Next, we will discuss the computation of the saturation.

We will consider a multi-continuum version of the method. Assume that an approximation of the velocity  $u_{ms}$  has been computed by the MGMsFEM. We derive the upscaled system following the ideas in Section 2.1. For each coarse element  $K_i$  and a continuum  $j$  within  $K_i$ , we solve the following system in an oversampled region  $K_i^+$ :

$$\nabla \cdot (u_{ms} \psi_i^j) + \mu = 0 \quad (27)$$

to obtain a basis function  $\psi_i^j$ . The above system is equipped with the constraints

$$\int_{K_m^{(l)}} \psi_i^j = \delta_{mj} \delta_{il}. \quad (28)$$

We remark that  $\mu$  is a piecewise constant function, and plays the role of Lagrange multiplier. We notice that the upscaled system has the form (9).

Now, we present some numerical examples. We take  $\Omega = [0, 1]^2$ , and the permeability field  $\kappa$  is shown in Figure 6. The coarse grid size  $H = 1/20$ . We will use a dual continuum model to solve this problem. For each coarse element  $K_j$ , we define two continua by  $K_j^{(1)} = \{x \in K_j | \kappa(x) > 10^3\}$  and  $K_j^{(2)} = \{x \in K_j | \kappa(x) \leq 10^3\}$ . In Table 2, we present a error comparison at times  $T = 5$  and  $T = 10$  between our method and the finite volume method for the saturation equation (26) with piecewise constant test functions in each continuum. From the table, we observe the performance of our scheme for various choices of oversampling layers. For all these cases, we observe that our scheme performs better than the usual (dual continuum) finite volume scheme whose error is 13.10% and 14.04% at the observation times  $T = 5$  and  $T = 10$  respectively. We notice that the relative error in the velocity  $u_{ms}$  is 5.51%. In Figure 7 - 8, we present the comparisons between the the averaged fine-grid solution and the solution obtained our proposed method. From these figures, we observe that our proposed method can capture the solution features accurately.

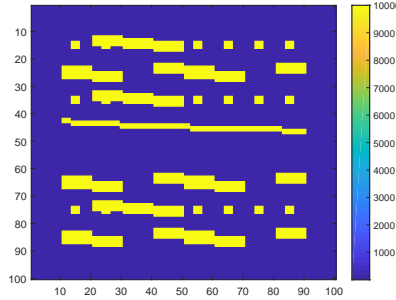


Figure 6: permeability field  $\kappa$

#layer \ time	$T = 5$	$T = 10$
4	12.83%	14.57%
6	7.33%	6.93%
8	5.89%	5.51%
$\infty$	5.69%	5.24%

Table 2:  $L^2$  relative errors for our upscaling method. The relative error for dual continuum finite volume scheme on the same grid is 13.10% and 14.04% for  $T = 5$  and  $T = 10$  respectively. In this case, the relative error in velocity  $u_{ms}$  is 5.51%.

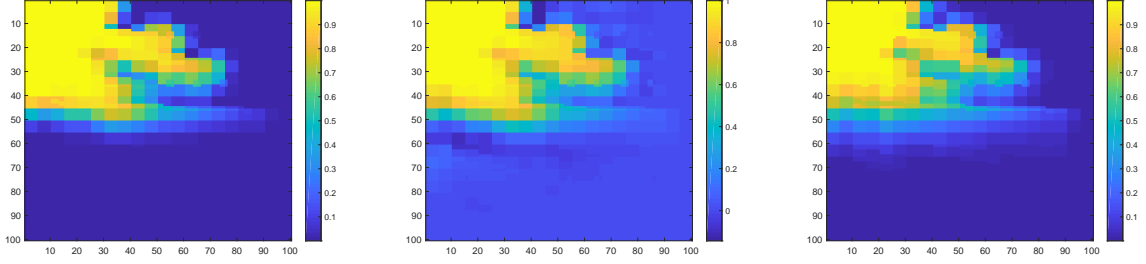


Figure 7: Snapshots of the solution at  $T = 10$ . Left: fine solution, Middle: upscaled solution, Right: finite volume solution.

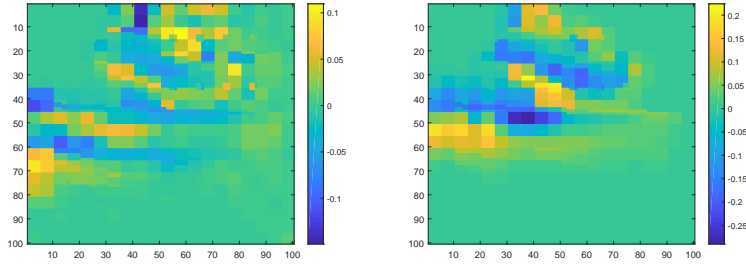


Figure 8: Error comparison to fine solution at  $T = 10$ . Left: upscaled solution, Right: finite volume solution.

### 4.3 Two phase flow

In this section, we apply our upscaling method to two phase flow problem which is described as follows:

$$\partial_t S_w + \nabla \cdot (u_w) = q_w, \quad (29)$$

$$-\nabla \cdot (\kappa \lambda_t(S_w) \nabla P_w) = q, \quad (30)$$

$$u_w = -\kappa \lambda_w(S_w) \nabla P_w, \quad (31)$$

$$\lambda_t = \lambda_w(S_w) + \lambda_o(S_w). \quad (32)$$

In the process of basis construction, we will use a similar approach as solving single phase flow problem. We notice that the exact velocity depends on the saturation and hence depends on time. To reduce the computational burden, we use the initial total mobility  $\lambda_t(S_w(0))$  as the reference mobility to construct the multiscale basis functions. That is, we will construct the multiscale basis functions for approximating the exact velocity field based on the following equations,

$$-\nabla \cdot (u_t) = q, \quad (33)$$

$$u_t = -\kappa \lambda_t(S_w(0, \cdot)) \nabla P. \quad (34)$$

Next, using the total velocity  $u_t$ , we will construct the basis functions for approximating the exact saturation based on the following transport equation,

$$\partial_t S_w + \nabla \cdot \left( \frac{u_t}{\lambda_t(S_w(0, \cdot))} S_w \right) = q_w, \quad (35)$$

Hence, the construction for the basis functions is separated into two parts. The first part is computing an approximating velocity  $u_{t,ms}^{(0)}$  and pressure  $P_{ms}$  by solving Equations (33) and (34) by Mixed Generalized Multiscale Finite Element Methods (MGMsFEM). The multiscale basis functions constructed during the processing are used to span the finite element space  $V_{ms}$ , which is used to approximate the exact velocity.

The second part is constructing the saturation basis functions by the method discussed in Section 3 with a fixed velocity  $u_{t,ms}^{(0)}$ . This part is also similar to the single phase flow.

To compute the coarse grid solution, we will use IMPLICIT Pressure Explicit Saturation (IMPES) scheme. Given the saturation  $S_{ms}^{(n)}$  and the total velocity  $u_{t,ms}^{(n)}$  at the previous time step, we will compute the total velocity at the next time step  $u_{t,ms}^{(n+1)}$  by solving

$$\int_{\Omega} \nabla \cdot u_{t,ms}^{(n+1)} p = \int_{\Omega} qp, \quad \forall p \in Q_H$$

$$\int_{\Omega} \kappa^{-1} \lambda_t^{-1}(S_w^{(n)}(\cdot, \cdot)) u_{t,ms}^{(n+1)} \cdot v = \int_{\Omega} P_{ms}^{(n+1)}, \nabla \cdot v, \quad \forall v \in V_{ms}$$

where  $Q_H$  is the space for pressure. Then, we will use the velocity  $u_{t,ms}^{(n+1)}$  to compute the saturation at the next time step as before (similar to (27) and (28)).

We next present some numerical examples. We take  $\Omega = [0, 1]^2$ . The permeability field  $\kappa$  is shown in Figure 9, and we use

$$\lambda_w = \left( \frac{S_w - S_{wc}}{1 - S_{wc} - S_{or}} \right)^2 \mu_w^{-1}, \quad \lambda_o = \left( \frac{1 - S_w - S_{or}}{1 - S_{wc} - S_{or}} \right)^2 \mu_o^{-1}$$

with  $\mu_w = 1$ ,  $\mu_o = 1$ ,  $S_{wc} = 0.2$  and  $S_{or} = 0.2$ . The coarse grid size  $H = 1/20$ . We are using the dual continuum model to solve this problem. For each coarse element  $K_j$ , we define two continua by  $K_j^{(1)} = \{x \in K_j | \kappa(x) > 10^3\}$  and  $K_j^{(2)} = \{x \in K_j | \kappa(x) \leq 10^3\}$ . In Table 3, we present a error comparison between our method and the finite volume method for the saturation equation with piecewise constant test functions in each continuum. For this experiment, we observed that the upscaling method works in general better than the finite volume method as before.

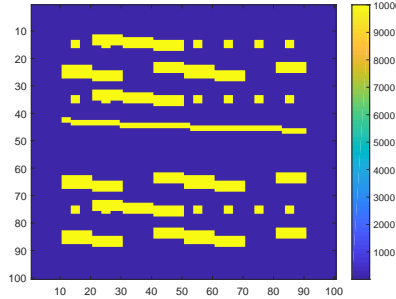


Figure 9: permeability field  $\kappa$

#layer \ time	$T = 10$	$T = 20$
4	15.82%	14.94%
6	7.03%	6.63%
8	4.11%	4.33%
$\infty$	3.52%	4.11%

Table 3:  $L^2$  relative errors for our upscaling method. The relative error for dual continuum finite volume scheme on the same grid is 10.01% and 14.13% for  $T = 10$  and  $T = 20$  respectively.

Next we consider another test case with the medium  $\kappa$  shown in Figure 10, which is a SPE benchmark test case. The coarse grid size is chosen as  $H = 1/24$ . We are again using the dual continuum model to solve this problem. For each coarse element  $K_j$ , we define  $K_j^{(1)} = \{x \in K_j | \log_{10}(\kappa(x)) > 0.8\}$  and  $K_j^{(2)} = \{x \in K_j | \log_{10}(\kappa(x)) \leq 0.8\}$ . In Figure 11, we present the snapshots of the averaged fine solution,

finite volume solution and our upscaled solution at the observation time  $T = 10$ . We observe that our method is able to capture the dynamics of the solution, while the finite volume method does not produce a good solution. In Table 4, we present the errors of our approximation and observe again good accuracy.

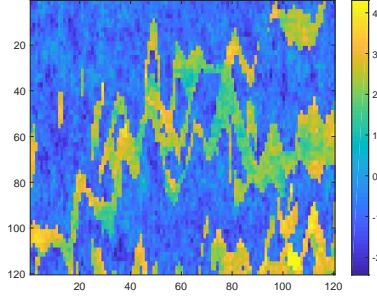


Figure 10: A SPE permeability field  $\log_{10}(\kappa)$  (in log scale).

#layer \ time	$T = 5$	$T = 10$
6	7.19%	11.12%
$\infty$	6.70%	10.16%

Table 4:  $L^2$  relative errors for our upscaling method. The relative error for dual continuum finite volume scheme on the same grid is 14.75% and 19.74% for  $T = 5$  and  $T = 10$  respectively.

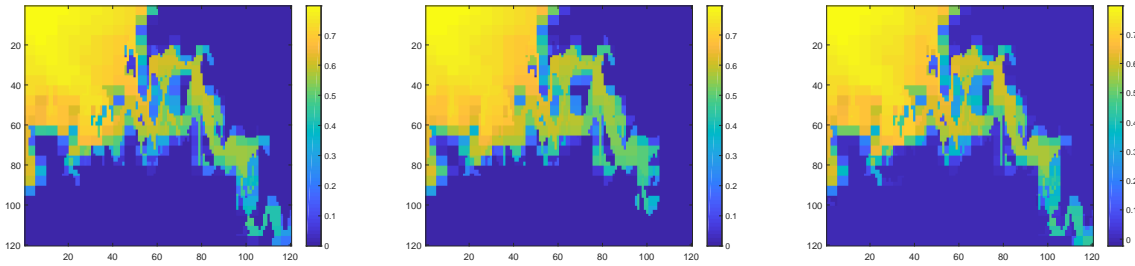


Figure 11: Snapshots of the solution at  $T = 10$ . Left: averaged fine solution. Middle: finite volume. Right: our upscaled solution.

## 5 Nonlinear Approach

In this section, we will present a numerical test to show the performance of the nonlinear approach (c.f. Section 3). To do, we consider the following single phase flow problem

$$\begin{aligned} \partial_t S_w + \nabla \cdot (u_w \lambda(S_w)) &= q_w, \\ -\nabla \cdot (\kappa \nabla P_w) &= q, \\ u_w &= -\kappa \nabla P_w, \end{aligned}$$

where

$$\lambda(S) = S^\beta.$$

We assume  $q$  is a function independent of time such that we can compute the velocity in the initial time step and use the velocity to construct the basis function for saturation.



The derivation of the upscaled system follows the ideas in Section 3.2. Assume that an approximation of the velocity  $u_{ms}$  has been computed. Let  $\{S_i^{n,j}\}$  be a set of upscaled values for the continuum  $j$  in the coarse region  $K_i$  at the time  $t_n$ . For each coarse element  $K_i$ , we solve the following system in an oversampled region  $K_i^+$ :

$$\nabla \cdot (u_{ms} \lambda(N_i)) + \mu = 0 \quad (36)$$

to obtain a local downscale function  $N_i$ . The above system is equipped with the constraints

$$\frac{1}{|K_i^{(j)}|} \int_{K_i^{(j)}} N_i = S_i^{n,j}. \quad (37)$$

We remark that  $\mu$  is a piecewise constant function, and plays the role of Lagrange multiplier. Then we define a global downscale field by

$$S_h^n = \sum_i N_i \chi^{K_i^+},$$

where  $\{\chi^{K_i^+}\}$  is a set of partition of unity functions corresponding to the sets  $K_i^+$ . Then we apply a finite volume scheme to the saturation equation as follows

$$S_i^{n+1,j} = S_i^{n,j} - \Delta t \int_{\partial K_i^{(j)}} \lambda(S_h^n) u_{ms} \cdot n + \Delta t \int_{K_i^{(j)}} q_w. \quad (38)$$

We notice that the upscaled system (38) has the form (17).

We next present some numerical results. We take  $\Omega = [0, 1]^2$ , and the permeability field  $\kappa$  is shown in Figure 12. The coarse grid size  $H = 1/10$ . We are using a dual continuum model to solve this problem. For each  $K_j$ , we define  $K_j^{(1)} = \{x \in K_j | \kappa(x) > 10^3\}$  and  $K_j^{(2)} = \{x \in K_j | \kappa(x) \leq 10^3\}$ . In Table 5, we present a error comparison between our method and the finite volume method for the saturation equation with piecewise constant test functions in each continua. We consider three choices of  $\beta$ , and present the relative errors at times  $T = 5$  and  $T = 10$ . From the results, we observe that our method is able to compute more accurate numerical solutions.

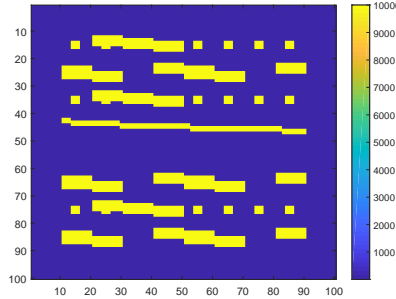


Figure 12: permeability field  $\kappa$

$\beta \setminus \text{time}$	$T = 5$	$T = 10$	$\beta \setminus \text{time}$	$T = 5$	$T = 10$
2	9.91%	11.85%	2	28.70%	23.61%
3	7.54%	12.60%	3	31.32%	26.27%
5	10.07%	14.89%	5	32.98%	29.19%

Table 5:  $L^2$  norm relative errors. Left: Nonlinear upscaling. Right: Finite volume method.

We remark that our proposed upscaling method can be applied to other nonlinear systems, which will be investigated in more detail in a forthcoming paper.

## 6 Conclusions

In this paper, we study and develop a general framework for coarse-grid modeling of nonlinear PDEs. The fine-grid problem is described by nonlinear PDEs including two-phase flow and transport model. The main concept of our upscaled model is three fold, (1) We determine macroscopic quantities in each coarse-grid block, which can vary among the coarse-grid blocks. (2) We define appropriate local problems with constraints in oversampled regions which are solvable. The constraints are given by macroscopic quantities. These local problems allow downscaling from macroscopic quantities to each coarse-grid block. (3) We formulate the coarse-grid problem such that the downscaled solution over the entire domain solves the global problem in a weak sense.

The formulation of local problems allow easily defining macroscopic fluxes. The local problems are defined via forcing terms. We also discuss the use of multiscale basis function in a linear fashion for solving nonlinear PDEs. Our main example includes two-phase flow and transport and its simplifications. The model problem is described by a coupled PDEs. We consider various permeability fields and show that one can achieve an accurate approximation of the solution.

## Acknowledgements

EC's work is partially supported by Hong Kong RGC General Research Fund (Project 14304217) and CUHK Direct Grant for Research 2017-18. EC would like to thank the support of the ESI for attending the program Numerical Analysis of Complex PDE Models in the Sciences.

## References

- [1] Assyr Abdulle and Yun Bai. Adaptive reduced basis finite element heterogeneous multiscale method. *Comput. Methods Appl. Mech. Engrg.*, 257:203–220, 2013.
- [2] G. Allaire and R. Brizzi. A multiscale finite element method for numerical homogenization. *SIAM J. Multiscale Modeling and Simulation*, 4(3):790–812, 2005.
- [3] T. Arbogast. Implementation of a locally conservative numerical subgrid upscaling scheme for two-phase Darcy flow. *Comput. Geosci*, 6:453–481, 2002.
- [4] T. Arbogast, G. Pencheva, M.F. Wheeler, and I. Yotov. A multiscale mortar mixed finite element method. *SIAM J. Multiscale Modeling and Simulation*, 6(1):319–346, 2007.
- [5] T. Arbogast, G. Pencheva, M.F. Wheeler, and I. Yotov. A multiscale mortar mixed finite element method. *Multiscale Model. Simul.*, 6(1):319–346, 2007.
- [6] GI Barenblatt, Iu P Zheltov, and IN Kochina. Basic concepts in the theory of seepage of homogeneous liquids in fissured rocks [strata]. *Journal of applied mathematics and mechanics*, 24(5):1286–1303, 1960.
- [7] J.W. Barker and S. Thibeau. A critical review of the use of pseudorelative permeabilities for upscaling. *SPE Reservoir Eng.*, 12:138–143, 1997.
- [8] Donald L Brown and Daniel Peterseim. A multiscale method for porous microstructures. *arXiv preprint arXiv:1411.1944*, 2014.
- [9] Y. Chen, L. Durllofsky, M. Gerritsen, and X. Wen. A coupled local-global upscaling approach for simulating flow in highly heterogeneous formations. *Advances in Water Resources*, 26:1041–1060, 2003.
- [10] E. Chung, Y. Efendiev, and S. Fu. Generalized multiscale finite element method for elasticity equations. *International Journal on Geomathematics*, 5(2):225–254, 2014.
- [11] E. Chung, Y. Efendiev, and C. Lee. Mixed generalized multiscale finite element methods and applications. *SIAM Multiscale Model. Simul.*, 13:338–366, 2014.

- [12] E. Chung, Y. Efendiev, and W. T. Leung. Generalized multiscale finite element method for wave propagation in heterogeneous media. *SIAM Multiscale Model. Simul.*, 12:1691–1721, 2014.
- [13] E. Chung and W. T. Leung. A sub-grid structure enhanced discontinuous galerkin method for multiscale diffusion and convection-diffusion problems. *Communications in Computational Physics*, 14:370–392, 2013.
- [14] E. T. Chung, Y. Efendiev, W.T. Leung, M. Vasilyeva, and Y. Wang. Online adaptive local multiscale model reduction for heterogeneous problems in perforated domains. *Applicable Analysis*, 96(12):2002–2031, 2017.
- [15] E. T. Chung, Y. Efendiev, and G. Li. An adaptive GMsFEM for high contrast flow problems. *J. Comput. Phys.*, 273:54–76, 2014.
- [16] Eric Chung, Yalchin Efendiev, and Wing Tat Leung. Constraint energy minimizing generalized multiscale finite element method in the mixed formulation. *Computational Geosciences*, 22(3):677–693, 2018.
- [17] Eric Chung, Maria Vasilyeva, and Yating Wang. A conservative local multiscale model reduction technique for stokes flows in heterogeneous perforated domains. *Journal of Computational and Applied Mathematics*, 321:389–405, 2017.
- [18] Eric T Chung, Efendiev, Wing Tat Leung, Maria Vasilyeva, and Yating Wang. Non-local multi-continua upscaling for flows in heterogeneous fractured media. *arXiv preprint arXiv:1708.08379*, 2018.
- [19] Eric T Chung, Yalchin Efendiev, and Wing Tat Leung. Constraint energy minimizing generalized multiscale finite element method. *Computer Methods in Applied Mechanics and Engineering*, 339:298–319, 2018.
- [20] Eric T Chung, Yalchin Efendiev, and Wing Tat Leung. Fast online generalized multiscale finite element method using constraint energy minimization. *Journal of Computational Physics*, 355:450–463, 2018.
- [21] Martin Drohmann, Bernard Haasdonk, and Mario Ohlberger. Reduced basis approximation for nonlinear parametrized evolution equations based on empirical operator interpolation. *SIAM J. Sci. Comput.*, 34(2):A937–A969, 2012.
- [22] L.J. Durlofsky. Numerical calculation of equivalent grid block permeability tensors for heterogeneous porous media. *Water Resour. Res.*, 27:699–708, 1991.
- [23] W. E and B. Engquist. Heterogeneous multiscale methods. *Comm. Math. Sci.*, 1(1):87–132, 2003.
- [24] Y. Efendiev and L.J. Durlofsky. Numerical modeling of subgrid heterogeneity in two phase flow simulations. *Water Resour. Res.*, 38(8):1128, 2002.
- [25] Y. Efendiev and L.J. Durlofsky. A generalized convection-diffusion model for subgrid transport in porous media. *SIAM J. Multiscale Modeling and Simulation*, 1(3):504–526, 2003.
- [26] Y. Efendiev, J. Galvis, and T. Y. Hou. Generalized multiscale finite element methods (gmsfem). *Journal of Computational Physics*, 251:116–135, 2013.
- [27] Y. Efendiev, J. Galvis, and X.H. Wu. Multiscale finite element methods for high-contrast problems using local spectral basis functions. *Journal of Computational Physics*, 230:937–955, 2011.
- [28] Y. Efendiev and T. Hou. *Multiscale Finite Element Methods: Theory and Applications*, volume 4 of *Surveys and Tutorials in the Applied Mathematical Sciences*. Springer, New York, 2009.
- [29] Y. Efendiev and A. Pankov. Numerical homogenization of monotone elliptic operators. *SIAM J. Multiscale Modeling and Simulation*, 2(1):62–79, 2003.
- [30] Y. Efendiev and A. Pankov. Numerical homogenization of nonlinear random parabolic operators. *SIAM J. Multiscale Modeling and Simulation*, 2(2):237–268, 2004.

- [31] Y. Efendiev and A. Pankov. Homogenization of nonlinear random parabolic operators. *Advances in Differential Equations*, 10(11):1235–1260, 2005.
- [32] DA Fafalis, SP Filopoulos, and GJ Tsamasphyros. On the capability of generalized continuum theories to capture dispersion characteristics at the atomic scale. *European Journal of Mechanics-A/Solids*, 36:25–37, 2012.
- [33] Dimitrios Fafalis and Jacob Fish. Computational continua for linear elastic heterogeneous solids on unstructured finite element meshes. *International Journal for Numerical Methods in Engineering*, 115(4):501–530, 2018.
- [34] Jacob Fish. *Practical multiscaleing*. John Wiley & Sons, 2013.
- [35] Jacob Fish and Wen Chen. Space–time multiscale model for wave propagation in heterogeneous media. *Computer Methods in applied mechanics and engineering*, 193(45):4837–4856, 2004.
- [36] Jacob Fish and Rong Fan. Mathematical homogenization of nonperiodic heterogeneous media subjected to large deformation transient loading. *International Journal for numerical methods in engineering*, 76(7):1044–1064, 2008.
- [37] Jacob Fish, Vasilina Filonova, and Dimitrios Fafalis. Computational continua revisited. *International Journal for Numerical Methods in Engineering*, 102(3-4):332–378, 2015.
- [38] Jacob Fish, Vasilina Filonova, and Zheng Yuan. Reduced order computational continua. *Computer Methods in Applied Mechanics and Engineering*, 221:104–116, 2012.
- [39] Jacob Fish and Sergey Kuznetsov. Computational continua. *International Journal for Numerical Methods in Engineering*, 84(7):774–802, 2010.
- [40] Jacob Fish, Kamlun Shek, Muralidharan Pandheeradi, and Mark S Shephard. Computational plasticity for composite structures based on mathematical homogenization: Theory and practice. *Computer Methods in Applied Mechanics and Engineering*, 148(1-2):53–73, 1997.
- [41] Jacob Fish and Zheng Yuan. Multiscale enrichment based on partition of unity. *International Journal for Numerical Methods in Engineering*, 62(10):1341–1359, 2005.
- [42] Jacob Fish and Zheng Yuan. Multiscale enrichment based on partition of unity for nonperiodic fields and nonlinear problems. *Computational Mechanics*, 40(2):249–259, 2007.
- [43] Patrick Henning and Mario Ohlberger. The heterogeneous multiscale finite element method for elliptic homogenization problems in perforated domains. *Numerische Mathematik*, 113(4):601–629, 2009.
- [44] L. Holden and B.F. Nielsen. Global upscaling of permeability in heterogeneous reservoirs: the Output Least Squares (OLS method). *Transport in Porous Media*, 40:115–143, 2000.
- [45] J.R. Kyte and D.W. Berry. New pseudofunctions to control numerical dispersion. *Society of Petroleum Engineers Journal*, 15(4):269–276, 1975.
- [46] Seong H Lee, MF Lough, and CL Jensen. Hierarchical modeling of flow in naturally fractured formations with multiple length scales. *Water resources research*, 37(3):443–455, 2001.
- [47] Ana-Maria Matache and Christoph Schwab. Two-scale fem for homogenization problems. *ESAIM: Mathematical Modelling and Numerical Analysis*, 36(04):537–572, 2002.
- [48] Caglar Oskay and Jacob Fish. Eigendefor-mation-based reduced order homogenization for failure analysis of heterogeneous materials. *Computer Methods in Applied Mechanics and Engineering*, 196(7):1216–1243, 2007.
- [49] H. Owhadi and L. Zhang. Metric-based upscaling. *Comm. Pure. Appl. Math.*, 60:675–723, 2007.

- [50] GP Panasenko. Multicontinuum wave propagation in a laminated beam with contrasting stiffness and density of layers. *Journal of Mathematical Sciences*, pages 1–13, 2018.
- [51] A. Pankov. *G-convergence and homogenization of nonlinear partial differential operators*. Kluwer Academic Publishers, Dordrecht, 1997.
- [52] M. Peszyńska, M. Wheeler, and I. Yotov. Mortar upscaling for multiphase flow in porous media. *Comput. Geosci.*, 6(1):73–100, 2002.
- [53] JE Warren, P Jj Root, et al. The behavior of naturally fractured reservoirs. 1963.
- [54] X.H. Wu, Y. Efendiev, and T.Y. Hou. Analysis of upscaling absolute permeability. *Discrete and Continuous Dynamical Systems, Series B.*, 2:158–204, 2002.
- [55] Zheng Yuan and Jacob Fish. Multiple scale eigendeformation-based reduced order homogenization. *Computer Methods in Applied Mechanics and Engineering*, 198(21-26):2016–2038, 2009.